PLOS ONE

RESEARCH ARTICLE

Thermomechanical Fractional Model of TEMHD Rotational Flow

F. Hamza[1], A. Abd El-Latief[1]*, W. Khatan[2]

1 Department of Mathematics, Faculty of Science, University of Alexandria, Alexandria, Egypt, **2** Department of Mathematics, Faculty of Science, University of Damanhour, Damanhour, Egypt

* m.abdellatief@yahoo.com

Abstract

In this work, the fractional mathematical model of an unsteady rotational flow of Xanthan gum (XG) between two cylinders in the presence of a transverse magnetic field has been studied. This model consists of two fractional parameters α and β representing thermomechanical effects. The Laplace transform is used to obtain the numerical solutions. The fractional parameter influence has been discussed graphically for the functions field distribution (temperature, velocity, stress and electric current distributions). The relationship between the rotation of both cylinders and the fractional parameters has been discussed on the functions field distribution for small and large values of time.

Citation: Hamza F, Abd El-Latief A, Khatan W (2017) Thermomechanical Fractional Model of TEMHD Rotational Flow. PLoS ONE 12(1): e0168530. doi:10.1371/journal.pone.0168530

Editor: Ming Dao, Massachusetts Institute of Technology, UNITED STATES

Received: July 2, 2015

Accepted: November 15, 2016

Published: January 3, 2017

Data Availability Statement: All relevant data are within the paper and its Supporting Information files.

Funding: Alexandria University is the only funder of this research. The funder had no role in study design, data collection and analysis, decision to publish, or preparation of the manuscript.

Competing Interests: The authors have declared that no competing interests exist.

Introduction

In many engineering fields such as electrical, mechanical, and nuclear engineering, the study of the fluid flow coupled with heat transfer in rotating annuli has great importance in applications [1]. The rotating flow is applied in several industrial applications such as turbo-machines, thermal motors and especially in turbines. The inner rotating flow is used in revolving jets and devices of combustion in order to increase the mixture between the reagents, as well as to stabilize the flame or to obtain advantages of better mixing [2]. A non-Newtonian fluid has many models that are applied in order to discuss the behavior of different materials; such as, drilling mud, certain oils, greases, and blood [3]–[5]. The oil industry has a great attention to the flow of fluids in annular spaces, both in drilling, and the artificial lifting of oil [6]. The second grade fluids are the common non-Newtonian viscoelastic fluids in industrial fields, such as polymer solutions [7, 8]. Laplace transform has widely used to obtain the exact solution of unsteady Magneto-hydro-dynamics (MHD) for different types of flow [9]–[17]. Thermo-electric magneto-hydro-dynamics (TEMHD) theory was originally developed by Shercliff for direct application in a fusion environment [18]. The thermoelectric effect develops the current between a liquid metal and a container wall when there is a temperature gradient along the interface between them [19, 20].

Recently, fractional calculus has encountered a great success in the description of viscoelasticity [21]–[23]. This was achieved by replacing the time derivative of an integer order by its fractional one. This process now allows one to define precisely the non-integer order derivatives. The Generalized second-order fluid with fractional anomalous diffusion studied by Xu

et al. [24], while the fractional derivative to the constitutive relationship models of Maxwell viscoelastic fluid and second grade fluid had been studied by Wenchang et al. [25, 26]. Fractional Maxwell fluid was examined for unsteady Couette flow by Athar et al. [27]. The oscillating flows in a generalized second grade fluid was studied by Jamil et al. [28]. The second grade fluid flow between two cylinders was studied differently, considering the flow of such fluid [29, 30]. Sherief et al. derived the fractional order theory of thermoelasticity by using fractional calculus [31]. Sherief and Abd El Latief have solved 1D problems [32, 33], and 2D [34] in the context of this modified fractional theory. They also studied the effect of the fractional derivative parameter on fractional thermoelastic material with variable thermal conductivity [35]. Abd El-Latief and Khader applied this theory to a 1D problem for a half-space overlaid by a thick layer of a different materials [36]. Ezzat [37, 38] constructed a mathematical model of the TEMHD in the context of the fractional heat conduction equation by using the Taylor series expansion of time fractional order developed by Jumarie [39]. Hamza et al. [40] modified the generalized theory of thermoelasticity with two relaxation times to be of fractional order derivative.

Here, we will introduce a fractional thermomechanical model with two parameters α and β for an unsteady rotational flow of thermoelectric fluids in the presence of a transverse magnetic field. Numerical solutions are obtained in the Laplace transform domain. The solutions in the physical domain are obtained numerically by using the Laplace inversion process based on a Fourier-series expansion. The Numerical results for the functions field distribution are represented graphically for different values of α and β with small and large values of time t. These graphs are analyzed for the counter direction rotation of two cylinders from which we can observe the physical behavior of these thermomechanical fractional parameters.

Formulation of the problem

Consider an unsteady laminar flow of an incompressible thermoelectric generalized second grade viscoelastic fluid situated in the annular region between two infinite coaxial isolated circular cylinders of radii R_1 and R_2 ($R_2 > R_1$). Then the cylinders suddenly begin to rotate, about their common axis $r = 0$ in different directions with a thermal shock that is a function of time. The surfaces of the cylinders are taken to be traction free where a constant magnetic field of strength H_0 acts axially in z-direction. The magnetic Reynolds number is assumed to be so small that the induced magnetic field is neglected. Due to the formulation of the problem with cylindrical coordinates (r, ϕ, z), all variables field depend on r and t only in ϕ-direction; as illustrated in Fig 1.

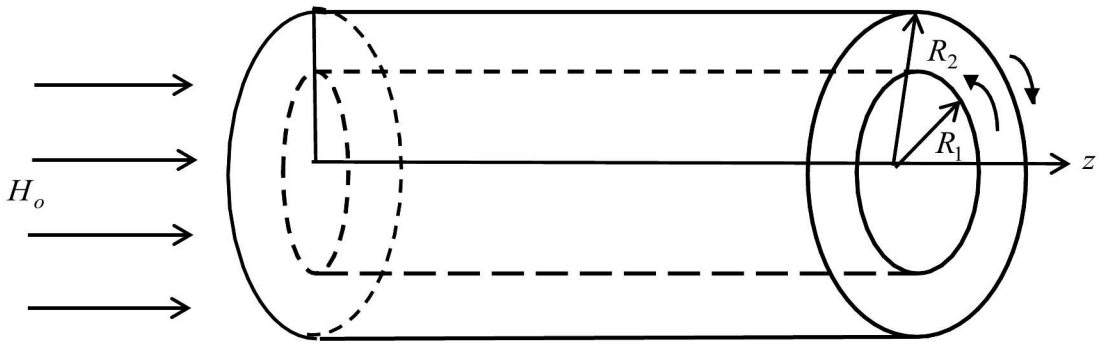

Fig 1. The geometry of the problem.

doi:10.1371/journal.pone.0168530.g001

To clarify the physical applications of the graph, the assumptions [41] are required in cylindrical coordinate as follow:

1. The fluid between the cylinders moves gradually with velocity $\boldsymbol{V} = (0, v(r, t), 0)$ while the constitutive equation of generalized second grade fluid, corresponding to this motion is given by [7]

$$\tau(r,t) = (\mu + \alpha_1 D_t^{\beta})\left(\frac{\partial}{\partial r} - \frac{1}{r}\right)v(r,t), \tag{1}$$

where $\tau(r, t) = T_{r\phi}$ is the non-zero shear stress, μ is the viscosity, α_1 is the first normal material modulus.

2. The modified Fourier law defined by Shercliff [18] for thermoelectric medium is extended using the Taylor series expansion of time fractional order would take the form [38]

$$\left(1 + \frac{\tau_0^{\alpha}}{\alpha!} D_t^{\alpha}\right)\boldsymbol{q} = -\kappa \nabla T + \pi_0 \boldsymbol{J}, \tag{2}$$

where κ is thermal conductivity, τ_0 is thermal relaxation time, $\boldsymbol{q}$ is heat conduction vector, T is the temperature and $\boldsymbol{J}$ is the current density vector given by the modified Ohm's law as follows;

$$\boldsymbol{J} = \sigma(\boldsymbol{E} + \boldsymbol{V} \times \boldsymbol{B} - k_0 \nabla T) \tag{3}$$

π_0 is the Peltier coefficient, k_0 is the Seebeck coefficient at reference temperature T_0 and σ is electrical conductivity. The electric intensity vector and the magnetic induction vector are $\boldsymbol{E}$, $\boldsymbol{B}$ respectively, where $\boldsymbol{B}$ has one constant non-vanishing component B_z which has the form;

$$B_z = \mu_0 H_0 = B_0 \tag{4}$$

3. The Lorentz force $\boldsymbol{F} = \boldsymbol{J} \times \boldsymbol{B}$, according to the above equations, has one component in ϕ-direction of the form:

$$F_{\phi} = -\sigma B_0^2 v + \sigma k_0 B_0 \frac{\partial T}{\partial r} \tag{5}$$

In the above assumptions, $D_t^{\alpha}, D_t^{\beta}$ are Caputo fractional time derivative operators of order α, β such that $0 < \alpha, \beta \leq 1$. Under these assumptions in the absence of polarization voltage, viscous dissipation, as well as heat source, and pressure gradient in the flow direction; the governing equations for such flow will take the form:

The energy equation

$$\rho c_p \frac{\partial}{\partial t}\left(1 + \frac{\tau_0^{\alpha}}{\alpha!} D_t^{\alpha}\right) T = (\kappa + \sigma \pi_0 k_0)\nabla^2 T - \sigma \pi_0 B_0 \left(\frac{1}{r}\frac{\partial}{\partial r}(rv)\right) \tag{6}$$

where ρ is density, c_p is specific heat at constant pressure and ∇^2 is Laplace operator given by $\nabla^2 = \frac{\partial^2}{\partial r^2} + \frac{1}{r}\frac{\partial}{\partial r}$.

The balance of the linear momentum leads to the relevant equation

$$\rho \frac{\partial v(r,t)}{\partial t} = \left(\frac{\partial}{\partial r} + \frac{2}{r}\right)\tau(r,t) + F_{\phi} \tag{7}$$

Eliminating $\tau(r, t)$ between Eqs (1) and (7), we get

$$\frac{\partial v}{\partial t} = \left(v + \frac{\alpha_1}{\rho} D_t^{\beta}\right)\left(\frac{\partial^2}{\partial r^2} + \frac{1}{r}\frac{\partial}{\partial r} - \frac{1}{r^2}\right)v - \frac{\sigma B_0^2}{\rho} v + \frac{\sigma k_0 B_0}{\rho}\frac{\partial T}{\partial r} \tag{8}$$

The boundary conditions are written as:

$$\begin{aligned} T(r,t) &= T_1 H(t), v(r,t) = \frac{v}{R_1} f(t) \quad t > 0, r = R_1 \\ T(r,t) &= T_2 H(t), v(r,t) = \frac{v}{R_1} g(t) \quad t > 0, r = R_2 \end{aligned} \tag{9}$$

where $H(t)$ is the Heaviside unit step function.

Let us introduce dimensionless variables.

$$\begin{aligned} v^* &= \frac{R_1}{v} v, r^* = \frac{r}{R_1}, t^* = \frac{v}{R_1^2} t, \tau_0^* = \frac{v}{R_1^2}\tau_0, \theta = \frac{T - T_0}{T_0} \\ &\alpha_1^* = \left(\frac{R_1^2}{v}\right)^{1-\beta} \alpha_1, J^* = \frac{R_1}{v\sigma B_0} J, \tau^* = \frac{R_1^2}{v\mu}\tau \end{aligned} \tag{10}$$

where $v = \frac{\mu}{\rho}$ is the kinematic viscosity.

Therefore, Eqs (6) and (8) are reduced to the non-dimensional forms (dropping the asterisk for convenience)

$$P_r \frac{\partial}{\partial t}\left(1 + \frac{\tau_0^{\alpha}}{\alpha!} D_t^{\alpha}\right)\theta = (1 + ZT_0)\nabla^2\theta - \Pi_0\left(\frac{1}{r}\frac{\partial}{\partial r}(rv)\right) \tag{11}$$

$$\frac{\partial v}{\partial t} = (1 + \eta D_t^{\beta})\left(\nabla^2 - \frac{1}{r^2}\right)v - M^2 v + K_0\frac{\partial \theta}{\partial r} \tag{12}$$

where; $P_r = \frac{c_p \mu}{\kappa}, M^2 = \frac{\sigma B_0^2 R_1^2}{\mu}, \eta = \frac{\alpha_1}{\rho R_1^2}, K_0 = \frac{\sigma k_0 B_0 T_0 R_1^2}{\mu v}, \Pi_0 = \frac{\pi_0 v \sigma B_0}{\kappa T_0}, ZT_0 = \frac{k_0^2 \sigma}{\kappa} T_0$

P_r, M^2, η are Prandtl number, Hartmann number and Viscoelastic parameter and ZT_0 is thermoelectric figure-of-merit [19]

Hence, the boundary condition in non-dimensional form will be

$$\begin{aligned} \theta(r,t) &= c_1 H(t), v(r,t) = f(t) \quad t > 0, r = 1 \\ \theta(r,t) &= c_2 H(t), v(r,t) = g(t) \quad t > 0, r = \ell \end{aligned} \tag{13}$$

where $c_1 = \frac{T_1}{T_0}, c_2 = \frac{T_2}{T_0}$ and $\ell = \frac{R_2}{R_1} > 1$.

Now consider the potential function Φ which is defined by [42]

$$v = \frac{\partial \Phi}{\partial r} \tag{14}$$

Substitute from Eq (14) into Eqs (11) and (12) and use the relation $\left(\nabla^2 - \frac{1}{r^2}\right)\frac{\partial f}{\partial r} = \frac{\partial}{\partial r}\nabla^2 f(r)$, we

get

$$P_r \frac{\partial}{\partial t}\left(1+\frac{\tau_0^\alpha}{\alpha!}D_t^\alpha\right)\theta = (1+ZT_0)\nabla^2\theta - \Pi_0\nabla^2\Phi \tag{15}$$

$$\frac{\partial\Phi}{\partial t} = (1+\eta D_t^\beta)\nabla^2\Phi - M^2\Phi + K_0\theta \tag{16}$$

Applying the Laplace transform with parameter s for both sides of Eqs (15) and (16) and using the homogenous initial condition [43], we obtain

$$P_r s\left(1+\frac{\tau_0^\alpha}{\alpha!}s^\alpha\right)\bar{\theta} = (1+ZT_0)\nabla^2\bar{\theta} - \Pi_0\nabla^2\bar{\Phi} \tag{17}$$

$$(s+M^2)\bar{\Phi} = (1+\eta s^\beta)\nabla^2\bar{\Phi} + K_0\bar{\theta} \tag{18}$$

The boundary conditions take the form

$$\begin{aligned} \bar{\theta}(r,s) &= \frac{c_1}{s}, \frac{\partial\bar{\Phi}}{\partial r} = F(s) \quad r=1 \\ \bar{\theta}(r,s) &= \frac{c_2}{s}, \frac{\partial\bar{\Phi}}{\partial r} = G(s) \quad r=\ell \end{aligned} \tag{19}$$

Now, we can rewrite Eqs (17) and (18) in the form

$$(\nabla^2 - a_1)\bar{\theta} = a_2\nabla^2\bar{\Phi} \tag{20}$$

$$(\nabla^2 - b_1)\bar{\Phi} = -b_2\bar{\theta} \tag{21}$$

where $a_1 = \frac{P_r s}{1+ZT_0}\left(1+\frac{\tau_0^\alpha}{\alpha!}s^\alpha\right)$, $a_2 = \frac{\Pi_0}{1+ZT_0}$, $b_1 = \frac{s+M^2}{1+\eta s^\beta}$ and $b_2 = \frac{K_0}{1+\eta s^\beta}$

Eliminating $\bar{\theta}$ between Eqs (20) and (21), we obtain the following fourth order differential equation satisfied by $\bar{\Phi}$

$$[\nabla^4 - (a_1+b_1-a_2b_2)\nabla^2 + a_1b_1]\bar{\Phi} = 0 \tag{22}$$

Eq (22) can be factorized as

$$(\nabla^2 - k_1^2)(\nabla^2 - k_2^2)\bar{\Phi} = 0 \tag{23}$$

where both k_1^2 and k_2^2 are the roots of the characteristic equation

$$k^4 - (a_1+b_1-a_2b_2)k^2 + a_1b_1 = 0 \tag{24}$$

The solution of Eq (23) can be written as

$$\bar{\Phi} = \sum_{i=1}^{2}\bar{\Phi}_i \tag{25}$$

where $\bar{\Phi}_i$ is the solution of equation

$$(\nabla^2 - k_i^2)\bar{\Phi} = 0, \mathrm{i} = 1,2 \tag{26}$$

Thus the general solution of Eq (23) has the form

$$\bar{\Phi} = \sum_{i=1}^{2}[A_i(s)I_0(k_i r) + B_i(s)K_0(k_i r)] \tag{27}$$

where $A_i(s)$ and $B_i(s)$, $i = 1, 2$ are parameters to be determined from the boundary conditions while $I_0(k_i r)$ and $K_0(k_i r)$ are the modified Bessel functions of the first and second kinds, respectively. By the same manner, we get

$$\bar{\theta} = \sum_{i=1}^{2}[C_i(s)I_0(k_i r) + N_i(s)K_0(k_i r)] \tag{28}$$

where $C_i(s)$ and $N_i(s)$, $i = 1, 2$ are parameters to be determined from the boundary conditions. The compatibility between Eqs (27), (28) and (21) gives

$$C_i = -\frac{k_i^2 - b_1}{b_2}A_i \tag{29}$$

$$N_i = -\frac{k_i^2 - b_1}{b_2}B_i \tag{30}$$

Substituting from Eqs (29) and (30) into Eq (28), we get

$$\bar{\theta} = -\frac{1}{b_2}\sum_{i=1}^{2}[A_i(k_i^2 - b_1)I_0(k_i r) + B_i(k_i^2 - b_1)K_0(k_i r)] \tag{31}$$

Using Eq (27) to determine the velocity, Eq (14), will take the form

$$\bar{v} = \sum_{i=1}^{2}[A_i k_i I_1(k_i r) - B_i k_i K_1(k_i r)] \tag{32}$$

Applying the Laplace transform for the non-dimensional form of Eq (1), we get

$$\bar{\tau} = (1 + \eta s^{\beta})\left(\frac{\partial}{\partial r} - \frac{1}{r}\right)\bar{v} \tag{33}$$

Using Eq (32) we obtain

$$\bar{\tau} = (1 + \eta s^{\beta})\sum_{i=1}^{2}\left\{A_i\left[k_i^2 I_0(k_i r) - \frac{2k_i}{r}I_1(k_i r)\right] + B_i\left[k_i^2 K_0(k_i r) + \frac{2k_i}{r}K_1(k_i r)\right]\right\} \tag{34}$$

The Laplace transform of the non-dimensional form of Eq (3) is given by

$$\bar{J} = \bar{v} - K_c\frac{\partial\bar{\theta}}{\partial r} \tag{35}$$

After substituting from Eqs (31) and (32) into Eq (35) and doing some manipulations, we obtain

$$\bar{J} = \sum_{i=1}^{2}\left\{k_i\left(1 + \frac{K_c}{b_2}(k_i^2 - b_1)\right)[A_i I_1(k_i r) - B_i K_1(k_i r)]\right\} \tag{36}$$

where $K_c = \frac{k_0 T_0}{\nu B_0}$

Using the boundary conditions Eq (19), we get

$$-\frac{1}{b_2}\sum_{i=1}^{2}[A_i(k_i^2-b_1)I_0(k_i)+B_i(k_i^2-b_1)K_0(k_i)]=\frac{c_1}{s} \tag{37}$$

$$-\frac{1}{b_2}\sum_{i=1}^{2}[A_i(k_i^2-b_1)I_0(k_i\ell)+B_i(k_i^2-b_1)K_0(k_i\ell)]=\frac{c_2}{s} \tag{38}$$

$$\sum_{i=1}^{2}[A_ik_iI_1(k_i)-B_ik_iK_1(k_i)]=F(s) \tag{39}$$

$$\sum_{i=1}^{2}[A_ik_iI_1(k_i\ell)-B_ik_iK_1(k_i\ell)]=G(s) \tag{40}$$

By solving the above system, the solution of the problem in the transformed domain could be obtained.

Inversion of the Laplace transforms

In order to invert the Laplace transform, we adopt a numerical inversion method based on a Fourier series expansion. By this method the Laplace inverse of the function $\bar{f}(s)$ is approximated by [44]

$$f(t)=\frac{\exp(ct)}{t_1}\left[\frac{1}{2}\bar{f}(c)+Re\sum_{k=1}^{N}\bar{f}\left(c+\frac{ik\pi}{t_1}\right)\exp\left(\frac{ik\pi t}{t_1}\right)\right],0<t<2t_1$$

where $i=\sqrt{-1}$, N is a sufficiently large integer representing the number of terms in the truncated Fourier series, chosen such that

$$\exp(ct)Re\left[\bar{f}\left(c+\frac{iN\pi}{t_1}\right)\exp\left(\frac{iN\pi t}{t_1}\right)\right]\leq\epsilon_1$$

where ϵ_1 is a prescribed small positive number that corresponds to the degree of accuracy required. The parameter c is a positive free parameter that must be greater than the real part of all the singularities of $\bar{f}(c)$. The optimal choice of c was obtained according to the criteria described in [44].

Numerical results and discussion

The polymer fluid chosen for purposes of numerical evaluations is 0.2% Xanthan Gum (XG) [45, 46]. XG solution has been used extensively in the oil industry for different applications due to its unique rheological properties. The experimental results indicate that fines generated during the drilling process form an external filter cake which in combination with XG results in considerable fluid loss reduction. The damage due to XG is small and limited to a narrow thickness around the wellbore [47]. The constants of the problem are shown in Table 1.

The computations were carried out for chosen functions $f(t) = -g(t) = H(t)$. The temperature, the velocity, the stress, and current density are calculated numerically using the inversion of Laplace transform outlined above. The FORTRAN programming language is used to solve the problem. The accuracy maintained is 6 digits in the numerical program.

Table 1. The constants of the problem.

$\eta = 0.805$	$M^2 = 0.25$	$\Pi_0 = 0.8$	$K_0 = 2$
$\tau_0 = 0.015$	$P_r = 0.71$	$K_c = 8$	$ZT_0 = 1$
$c_1 = 1$	$c_2 = 1$	$\ell = 2$	

doi:10.1371/journal.pone.0168530.t001

Figs (2–4) represent the variables field distributions namely, the temperature, the velocity and the stress, respectively. Each Figure split into four subfigures, part(a) describe the variation of the functions field with small times, namely, $t = 0.01, 0.09, 0.15, 0.2$ when $\alpha = \beta = 1$ while in part(b) the calculation is done for large values of time, namely, $t = 10, 20, 30, 40$ when $\alpha = \beta = 1$. Part(c), (d) illustrate the influence of the fractional parameters α, β respectively when $t = 0.2$.

We notice that the magnitude of temperature, velocity and stress were increased with the increasing time [30]. Also from Fig 2 Part(a) for the smallest value of time, the generalized theory with one relaxation time (G- theory) is prominent. This is in agreement with [48].

The rotation of the two cylinders divides the fluid region into two parts according to the direction of rotation. The first one is denoted by R_{in} in which the fluid rotates in the same direction as the inner cylinder while the second part is R_{out} due to the outer cylinder rotation. It is observed from Fig 3 Part(a) that as the time increases, the value of R_{in} and the peak of velocity increases, as shown in Table 2.

From Figs (2–4) part(b) it can be noticed that the functions field unchanging at large time $t = 10, 20, 30, 40$. This means that the steady state is achieved. For the steady state analysis, see S1 Text.

Figs (2–4) part(c) it is noticed that the magnitude of the fields distribution increases with the increase of α. Fig 3 Part(c) shows the α influence on R_{in} is insignificant while the peak of the velocity increases when α increases as shown in Table 3.

Figs (2–4) part(d) it is noticed that the magnitude of the temperature, the velocity, and the stress increase with the increasing of β. Fig 3 Part(d) shows the β influence on R_{in} and the peak are prominent but for viscous fluid ($\beta = 0$) the peak disappears (see Table 4).

From Fig 3 Part(a), (d) it has been observed that for small value of time the influences of the time t and the fractional parameter β on R_{in} are prominent. This region extended by increasing both of them until the interaction between R_{in} and R_{out} occurs (see S1 Video). Later the inner region returns back towards the inner cylinder (see S2 Video). This is due to the reaction of the fluid particles in the outer region on the inner region. Fig 4 Part(a), (c), (d) show the behavior of the stress distribution at small value of time which is compatible with recent work [30].

Fig 5(a)–5(d) depicts the variations of the temperature θ, the velocity v, the stress τ, and the current density J, respectively, at large values of time ($t = 20$, $t = 30$) for both Newtonian ($\eta = 0$) and non-Newtonian fluids ($\eta = 0.805$) at $\alpha = \beta = 1$.

It has been observed that for large times all the functions field are the same for the Newtonian and non-Newtonian fluids. This result is compatible with the physical phenomena that for a large time the steady state is achieved due to the viscosity of the fluid. Now, there is a question arises here; Is the change of the fraction parameters effect on the functions field distribution in the case of large values of time? The answer is obtained from Fig 6(a)–6(d).

This figure shows the functions field for large value of time, $t = 20$ as well as for different large values of α, β. It is noticed that the fractional parameters have no effect on all functions field. Hence mulling over Figs 5 and 6 we conclude that when steady state occurs the fractional parameters have no effect on all functions field (see S3 Video).

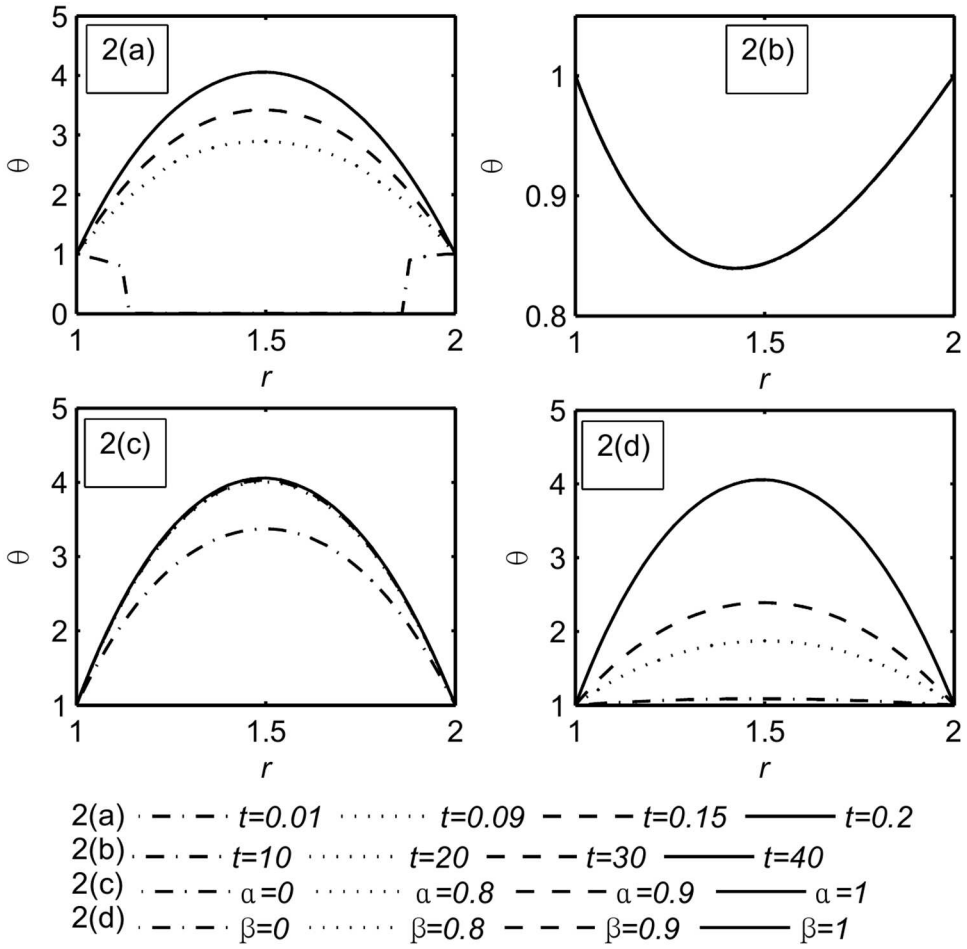

Fig 2. Temperature distribution θ. Part(a): For different values of small time, namely, $t = 0.01, 0.09, 0.15, 0.2$ when $\alpha = \beta = 1$. Part(b): For different values of large time, namely, $t = 10, 20, 30, 40$ when $\alpha = \beta = 1$. Part (c): For different values of α, namely, $\alpha = 0, 0.8, 0.9, 1$ when $t = 0.2$, $\beta = 1$. Part(d): For different values of β, namely, $\beta = 0, 0.8, 0.9, 1$ when $t = 0.2$, $\alpha = 1$.

doi:10.1371/journal.pone.0168530.g002

The influences of the physical parameters on all functions field at small and large value of times, namely, $t = 0.2$ and $t = 20$ are shown in S1–S8 Figs.

It is observed from S1 Fig that, for small values of time, the effect of increasing Prandtl number P_r is to decrease the values of the temperature, the velocity and the current. On the other hand the increase Prandtl number P_r tends to increase the value of the stress. The physical explanation of the above observation is that increasing P_r tends to decrease the thermal conductivity of the fluid resulting on a lower temperature. Also, increasing P_r increases the viscosity of the fluid producing higher stress values and slower speed [12]. We note that for large values of time (shown in S2 Fig) the Prandtl number P_r has no effect on all the functions. This result is compatible with the equations of the steady state which are independent of P_r.

From S3 Fig we conclude that increasing the thermoelectric parameter ZT_0 results in increasing the values of the velocity while decreasing the temperature and the stress. This is because increasing ZT_0 decreases the thermal conductivity and increases the Seebeck coefficient and electric conductivity. For large values of time (shown in S4 Fig) the effect of ZT_0 on

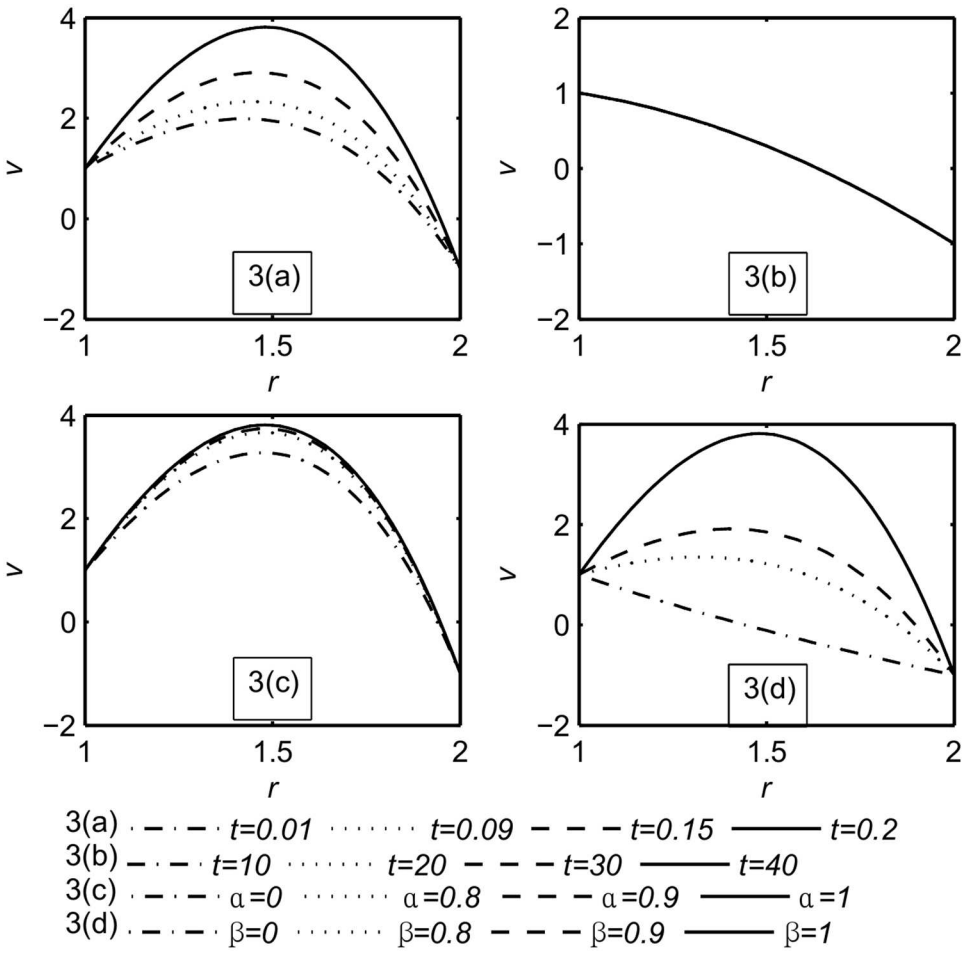

Fig 3. Velocity distribution *v*. Part(a): For different values of small time, namely, $t = 0.01, 0.09, 0.15, 0.2$ when $\alpha = \beta = 1$. Part(b): For different values of large time, namely, $t = 10, 20, 30, 40$ when $\alpha = \beta = 1$. Part(c): For different values of α, namely, $\alpha = 0, 0.8, 0.9, 1$ when $t = 0.2$, $\beta = 1$. Part(d): For different values of β, namely, $\beta = 0, 0.8, 0.9, 1$ when $t = 0.2$, $\alpha = 1$.

doi:10.1371/journal.pone.0168530.g003

the stress and on the current is most prominent while it has a small effect on the temperature and a very small effect on the velocity. The increase of ZT_0 decreases the values of the velocity while increasing the values of both the temperature and the stress. The effect on the current is not consistent due to the rotation of parts of the fluid in opposite directions.

We see from S5 Fig that the increase of the Hartmann number M^2 results in the increase of the values of the stress and a decrease in the values of both the temperature and the velocity. As before, the rotation of the fluid affects the current in different ways according to the direction of the rotating fluid. S6 Fig shows that for large values of time, the effect of the Hartmann number M^2 on the temperature, the velocity and the stress is the same (with different values) as in S5 Fig. The graph of the current shows that: it increases consistently with the increase of the Hartmann number. S7 and S8 Figs show that for small or large values of time, the parameter K_c, as expected from Eq (35), affects the current only and has no effect on the other functions.

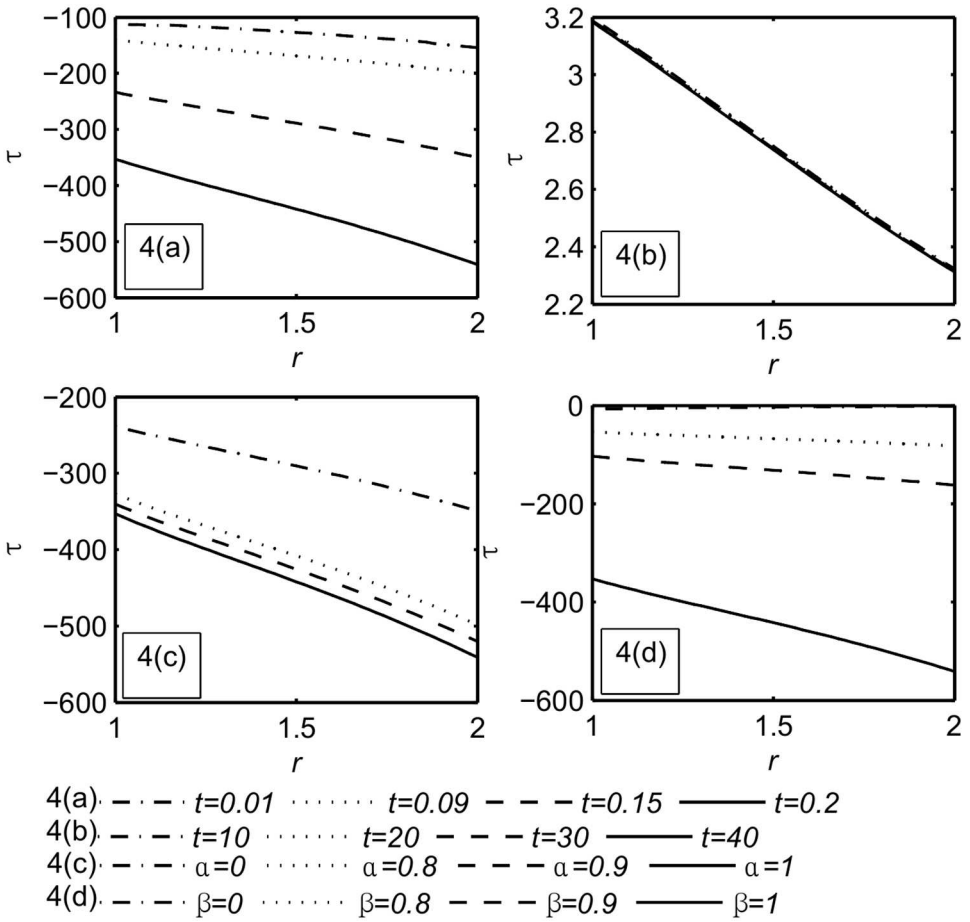

Fig 4. The stress distribution τ. Part(a): For different values of small time, namely, $t = 0.01, 0.09, 0.15, 0.2$ when $\alpha = \beta = 1$. Part(b): For different values of large time, namely, $t = 10, 20, 30, 40$ when $\alpha = \beta = 1$. Part(c): For different values of α, namely, $\alpha = 0, 0.8, 0.9, 1$ when $t = 0.2$, $\beta = 1$. Part(d): For different values of β, namely, $\beta = 0, 0.8, 0.9, 1$ when $t = 0.2$, $\alpha = 1$.

doi:10.1371/journal.pone.0168530.g004

Table 2. The influence of the inner region R_{in} and peak on the velocity at $\alpha = \beta = 1$ for different time t.

t	R_{in}	peak
0.01	1.898990	(1.424242, 1.988389)
0.09	1.909091	(1.444444, 2.331563)
0.15	1.929293	(1.464646, 2.907461)
0.2	1.939394	(1.484848, 3.809927)

doi:10.1371/journal.pone.0168530.t002

Conclusions

The present study describes the fractional mathematical model of an unsteady rotational flow of Xanthan gum (XG) between two cylinders in the presence of a transverse magnetic field. The cylinders rotate in a counter direction and affected with thermal shock that is function of time.

Table 3. The peak on the velocity at $\beta = 1$ and $t = 0.2$ for different fractional parameter α.

α	peak
0.0	(1.474747, 3.270884)
0.8	(1.474747, 3.665751)
0.9	(1.474747, 3.737811)
1	(1.474747, 3.809938)

doi:10.1371/journal.pone.0168530.t003

Table 4. The influence of the inner region R_{in} and peak on the velocity at $\alpha = 1$, $t = 0.2$ for different fractional parameter β.

β	R_{in}	peak
0.0	1.434343	Non
0.8	1.848485	(1.323232, 1.350466)
0.9	1.88889	(1.404040, 1.911008)
1	1.939394	(1.484848, 3.809927)

doi:10.1371/journal.pone.0168530.t004

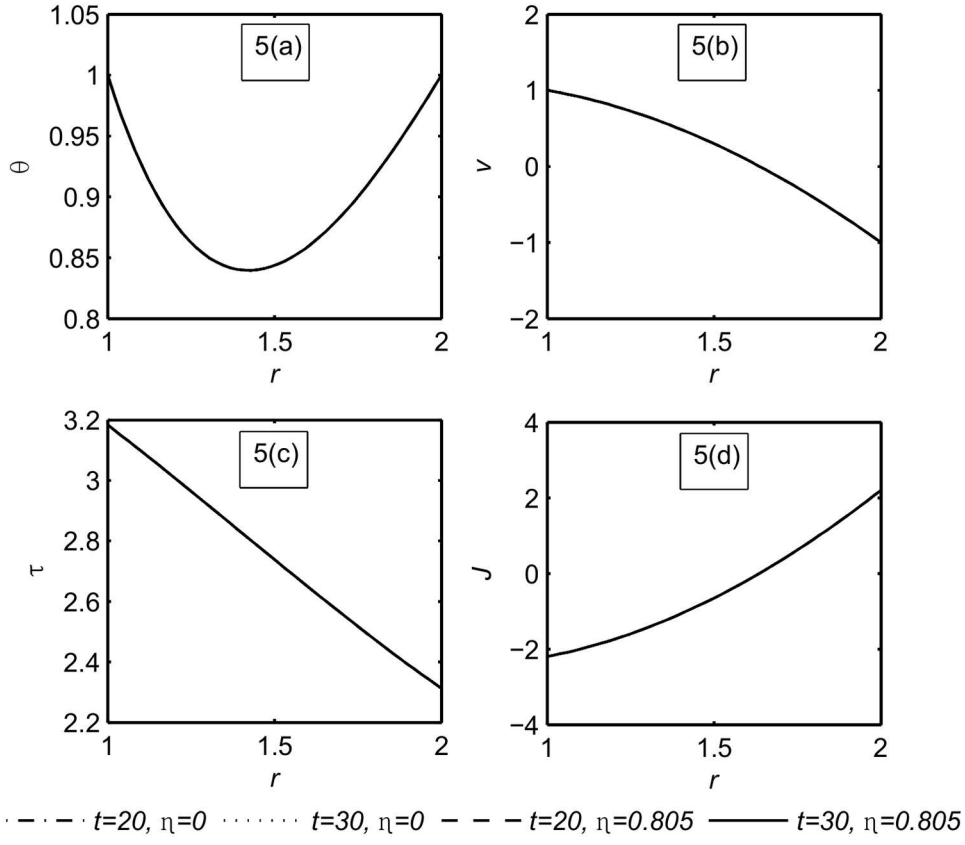

Fig 5. The functions field θ, v, τ, J at large time $t = 20$, $t = 30$ for both Newtonian ($\eta = 0$) and non-Newtonian fluid ($\eta = 0.805$) when $\alpha = \beta = 1$.

doi:10.1371/journal.pone.0168530.g005

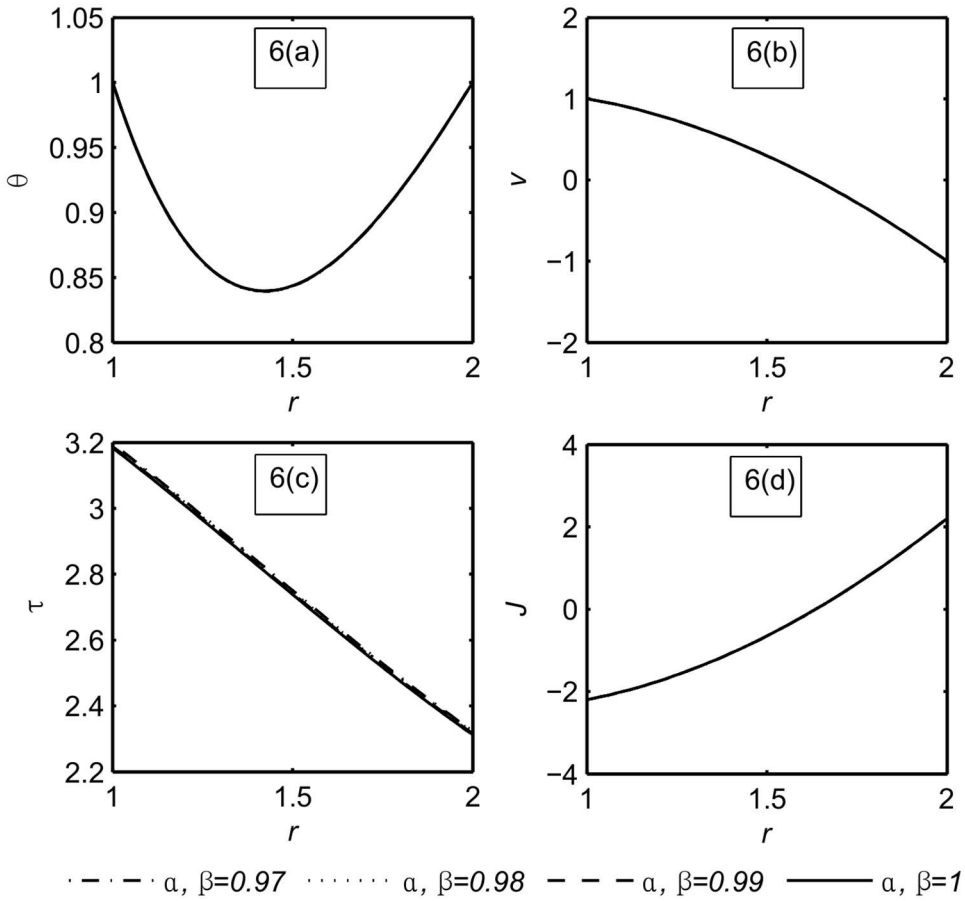

Fig 6. The functions field θ, v, τ, J at large time $t = 20$ and different large values of α, $\beta = 0.97, 0.98, 0.99, 1$.

doi:10.1371/journal.pone.0168530.g006

The summary of this study for different time intervals are as follow:

For small values of time

- In all related figures, it is noticed that the thermomechanical fractional parameters α and β have a significant effect on all fields.
- The fractional parameter β controls the rotation of the inner region R_{in} while the fractional parameter α has nuance effect on this region.
- The inner rotated region R_{in} extended by the time, as the fractional parameter β increases.
- In the presence of the applied magnetic field, the fluid motion is directly affected by the rotation of the inner cylinder more than the rotation of the outer cylinder.
- It has been found that; this model for small values of time, the temperature profile is in agreement with generalized theory of one relaxation time.

For large values of time

- Strong non-Newtonian effect is present for small value of time while for large times it becomes weak and behaves like a Newtonian fluid.
- The change of the fractional parameters α, β has no considerable effect on the functions field.

Supporting Information

S1 Video. 3D simulation of the fractional parameter effects on the two coaxial rotating cylinders for small value of time. This video explains the movement of the inner fluid region R_{in} where its boundary is represented by a moving blue cylinder for different values of the fractional parameter β. It is observed that after a certain duration of time, this region is extended towards the outer cylinder as the fractional parameters increase.
(AVI)

S2 Video. 3D simulation of the time effects on the two coaxial rotating cylinders after interaction occurs. After the interaction of the fluid regions occur, the inner flow returns back towards the inner cylinder. This is due to the reaction of the fluid particles in the outer region on the particles in the inner region.
(AVI)

S3 Video. 3D simulation of the time effects on the two coaxial rotating cylinders for large value of time. In this case, the steady state occurs and the Non-Newtonian fluid behaves like Newtonian one whatever the value of α and β.
(AVI)

S1 Text. Steady state analysis. This text contains some more detailed information about the functions field at large value of time t where the steady state is achieved.
(DOC)

S1 Fig. The influence of P_r on all functions field at small value of time. The functions field θ, v, τ, J at small time $t = 0.2$ and different values of Prandtl number $P_r = 0.5, 0.6, 0.71, 0.8$.
(PDF)

S2 Fig. The influence of P_r on all functions field at large value of time. The functions field θ, v, τ, J at large time $t = 20$ and different values of Prandtl number $P_r = 0.5, 0.6, 0.71, 0.8$.
(PDF)

S3 Fig. The influence of ZT_0 on all functions field at small value of time. The functions field θ, v, τ, J at small time $t = 0.2$ and different values of Thermoelectric figure-of-merit $ZT_0 = 1, 1.5, 1.7, 2$.
(PDF)

S4 Fig. The influence of ZT_0 on all functions field at large value of time. The functions field θ, v, τ, J at large time $t = 20$ and different values of Thermoelectric figure-of-merit $ZT_0 = 1, 1.5, 1.7, 2$.
(PDF)

S5 Fig. The influence of M^2 on all functions field at small value of time. The functions field θ, v, τ, J at small time $t = 0.2$ and different values of Hartmann number $M^2 = 0, 0.25, 0.5, 1$.
(PDF)

S6 Fig. The influence of M^2 on all functions field at large value of time. The functions field θ, v, τ, J at large time $t = 20$ and different values of Hartmann number $M^2 = 0, 0.25, 0.5, 1$.
(PDF)

S7 Fig. The influence of K_c on all functions field at small value of time. The functions field θ, v, τ, J at small time $t = 0.2$ and different values of K_c, namely, $K_c = 0.2, 0.8, 2, 8$.
(PDF)

S8 Fig. The influence of K_c on all functions field at large value of time. The functions field θ, v, τ, J at large time $t = 20$ and different values of K_c, namely, $K_c = 0.2, 0.8, 2, 8$.
(PDF)

Acknowledgments

We would like to express our sincere appreciation for the academic Editor and reviewers for their helpful comments to improve the quality of this work. we are also thankful for Dr. A. Younes.

Author Contributions

Analyzed the data: FH AA WK.

Contributed reagents/materials/analysis tools: FH AA WK.

Wrote the paper: FH AA WK.

References

1. Sukumaran AK, Reji R, Santhosh K. Fluid flow simulations within rotating annulus. Proc. of the 37th Nat. & 4th Conf. on Fluid Mech. and Fluid Power. 2010 AM4: 1–10.
2. Owen JM, Zhou K, Pountney O, Wilson M, Lock G. Prediction of Ingress Through Turbine Rim Seals-Part I: Externally Induced Ingress. Journal of Turbomachinery. 2012 (134): 031012. doi: 10.1115/1.4003071
3. Asghar S, Mohyuddin MR, Hayat T. Effects of Hall current and heat transfer on flow due to a pull of eccentric rotating disks. International Journal of Heat and Mass Transfer. 2005 (48): 599–607. doi: 10.1016/j.ijheatmasstransfer.2004.08.023
4. Mohyuddin MR, Götz T. Resonance behaviour of viscoelastic fluid in Poiseuille flow in the presence of a transversal magnetic field. International Journal for numerical methods in fluids. 2005 (49): 837–847. doi: 10.1002/fld.1026
5. Fetecau C, Akhtar W, Imran M, Vieru D. On the oscillating motion of an Oldroyd-B fluid between two infinite circular cylinders. Computers & Mathematics with Applications. 2010 (59): 2836–2845. doi: 10.1016/j.camwa.2010.02.002
6. Pereira F, Ataíde C, Barrozo M. CFD Approach using a discrete phase model for annular flow analysis. Latin American applied research. 2010 (40): 53–60.
7. Sharma R, Bhargava A, Kumar N, Chandramouli A. Some Exact Solutions for Rotating Flows of a Generalized Second Grade Fluid in Cylindrical Domains. Journal of Pure and Applied Science & Technology. 2011 (1): 36–46.
8. Khajohnsaksumeth N, Wiwatanapataphee B, Wu YH. The effect of boundary slip on the transient pulsatile flow of a modified second-grade fluid. Abstract and Applied Analysis. 2013 (2013). doi: 10.1155/2013/858597
9. Ali F, Khan I, Mustapha N, Shafie S. Unsteady magnetohydrodynamic oscillatory flow of viscoelastic fluids in a porous channel with heat and mass transfer. Journal of the Physical Society of Japan. 2012 (81): 064402. doi: 10.1143/JPSJ.81.064402
10. Ali F, Khan I, Samiulhaq, Shafie S. Conjugate effects of heat and mass transfer on MHD free convection flow over an inclined plate embedded in a porous medium. PLoS One. 2013 (8): e65223. doi: 10.1371/journal.pone.0065223 PMID: 23840321

11. Khan A, Khan I, Ali F, Ulhaq S, Shafie S. Effects of wall shear stress on unsteady MHD conjugate flow in a porous medium with ramped wall temperature. PLoS One. 2014 (9): e90280. doi: 10.1371/journal.pone.0090280 PMID: 24621775
12. Hussanan A, Ismail Z, Khan I, Hussein AG, Shafie S. Unsteady boundary layer MHD free convection flow in a porous medium with constant mass diffusion and Newtonian heating. The European Physical Journal Plus. 2014 (129): 1–16. doi: 10.1140/epjp/i2014-14046-x
13. Samiulhaq, Ahmad S, Vieru D, Khan I, Shafie S. Unsteady magnetohydrodynamic free convection flow of a second grade fluid in a porous medium with ramped wall temperature. PLoS One. 2014 (9): e88766. doi: 10.1371/journal.pone.0088766 PMID: 24785147
14. Gul T, Islam S, Shah RA, Khan I, Khalid A, Shafie S. Heat transfer analysis of MHD thin film flow of an unsteady second grade fluid past a vertical oscillating belt. PLoS One. 2014 (9): e103843. doi: 10.1371/journal.pone.0103843 PMID: 25383797
15. Anwar M, Sharidan S, Khan I, Salleh M. Magnetohydrodynamic and radiation effects on stagnation-point flow of nanofluid towards a nonlinear stretching sheet. Indian Journal of Chemical Technology. 2014 (21): 199–204.
16. Khalid A, Khan I, Shafie S. Exact solutions for free convection flow of nanofluids with ramped wall temperature. The European Physical Journal Plus. 2015 (130): 1–14. doi: 10.1140/epjp/i2015-15057-9
17. Khalid A, Khan I, Khan A, Shafie S. Unsteady MHD free convection flow of Casson fluid past over an oscillating vertical plate embedded in a porous medium. Engineering Science and Technology, an International Journal. 2015:1–9.
18. Shercliff J. Thermoelectric magnetohydrodynamics. Journal of fluid mechanics. 1979 (91): 231–251. doi: 10.1017/S0022112079000136
19. Nemir D, Beck J. On the significance of the thermoelectric figure of merit Z. Journal of electronic materials. 2010 (39): 1897–1901. doi: 10.1007/s11664-009-1060-4
20. Ruzic DN, Xu W, Andruczyk D, Jaworski M. Lithium-metal infused trenches (LiMIT) for heat removal in fusion devices. Nucl Fusion. 2011 (51): 4. doi: 10.1088/0029-5515/51/10/102002
21. Tong D, Wang R,Yang H. Exact solutions for the flow of non-Newtonian fluid with fractional derivative in an annular pipe. Science in China Series G: Physics, Mechanics and Astronomy. 2005 (48): 485–495. doi: 10.1360/04yw0105
22. Shah SHAM. Some helical flows of a Burgers fluid with fractional derivative. Meccanica. 2010 (45): 143–151. doi: 10.1007/s11012-009-9233-z
23. Hemeda A. Solution of fractional partial differential equations in fluid mechanics by extension of some iterative method. Abstract and Applied Analysis. 2013 (2013): 1–9. doi: 10.1155/2013/717540
24. Xu M, Tan W. Theoretical analysis of the velocity field, stress field and vortex sheet of generalized second order fluid with fractional anomalous diffusion. Science in China Series A: Mathematics. 2001 (44): 1387–1399. doi: 10.1007/BF02877067
25. Wenchang T, Wenxiao P, Mingyu X. A note on unsteady flows of a viscoelastic fluid with the fractional Maxwell model between two parallel plates. International Journal of Non-Linear Mechanics. 2003 (38): 645–650. doi: 10.1016/S0020-7462(01)00121-4
26. Wenchang T, Mingyu X. Unsteady flows of a generalized second grade fluid with the fractional derivative model between two parallel plates. Acta Mechanica Sinica. 2004 (20): 471–476. doi: 10.1007/BF02484269
27. Athar M, Fetecau C, Kamran M, Sohail A, Imran M. Exact solutions for unsteady axial Couette flow of a fractional Maxwell fluid due to an accelerated shear. Nonlinear Analysis: Modelling and Control. 2011 (16): 135–151.
28. Jamil M, Khan NA, Rauf A. Oscillating flows of fractionalized second grade fluid. ISRN Mathematical Physics. 2012 (2012): 1–23. doi: 10.5402/2012/908386
29. Mahmood A, Parveen S, Khan NA. Exact solutions for the flow of second grade fluid in annulus between torsionally oscillating cylinders. Acta Mechanica Sinica. 2011 (27): 222–227. doi: 10.1007/s10409-011-0443-y
30. Imran M, Kamran M, Athar M, Zafar A. Taylor-Couette flow of a fractional second grade fluid in an annulus due to a time-dependent couple. Nonlinear Analysis: Modelling and Control. 2011 (16): 47–58.
31. Sherief HH, El-Sayed A, Abd El-Latief A. Fractional order theory of thermoelasticity. International Journal of Solids and structures. 2010 (47): 269–275. doi: 10.1016/j.ijsolstr.2009.09.034
32. Sherief HH, Abd El-Latief A. A one-dimensional fractional order thermoelastic problem for a spherical cavity. Mathematics and Mechanics of Solids. 2013.

33. Sherief HH, Abd El-Latief A. Application of fractional order theory of thermoelasticity to a 1D problem for a half-space. ZAMM-Journal of Applied Mathematics and Mechanics/Zeitschrift für Angewandte Mathematik und Mechanik. 2014 (94): 509–515. doi: 10.1002/zamm.201200173

34. Sherief HH, Abd El-Latief A. Application of fractional order theory of thermoelasticity to a 2D problem for a half-space. Applied Mathematics and Computation. 2014 (248): 584–592. doi: 10.1016/j.amc.2014.10.019

35. Sherief HH, Abd El-Latief A. Effect of variable thermal conductivity on a half-space under the fractional order theory of thermoelasticity. International Journal of Mechanical Sciences. 2013 (74): 185–189. doi: 10.1016/j.ijmecsci.2013.05.016

36. Abd El-Latief A, Khader S. Fractional model of thermoelasticity for a half-space overlaid by a thick layer. ZAMM-Journal of Applied Mathematics and Mechanics/Zeitschrift für Angewandte Mathematik und Mechanik. 2014. doi: 10.1002/zamm.201300174

37. Ezzat MA. Thermoelectric MHD non-Newtonian fluid with fractional derivative heat transfer. Physica B: Condensed Matter. 2010 (405): 4188–4194. doi: 10.1016/j.physb.2010.07.009

38. Ezzat MA. State space approach to thermoelectric fluid with fractional order heat transfer. Heat and Mass Transfer. 2012 (48): 71–82. doi: 10.1007/s00231-011-0830-8

39. Jumarie G. Derivation and solutions of some fractional Black-Scholes equations in coarse-grained space and time. Application to Merton's optimal portfolio. Computers & mathematics with applications. 2010 (59): 1142–1164. doi: 10.1016/j.camwa.2009.05.015

40. Hamza F, Abdou M, Abd El-Latief A. Generalized Fractional Thermoelasticity Associated with Two Relaxation Times. Journal of Thermal Stresses. 2014 (37): 1080–1098. doi: 10.1080/01495739.2014.936196

41. Hamza F, Abd El-Latief A, Khatan W. Thermomechanical Fractional Model of Two Immiscible TEMHD. Advances in Materials Science and Engineering. 2015 (2015). doi: 10.1155/2015/391454

42. Sherief HH, Anwar MN. A problem in generalized thermoelasticity for an infinitely long annular cylinder. International journal of engineering science. 1988 (26): 301–306. doi: 10.1016/0020-7225(88)90079-1

43. Podlubny I. Fractional differential equations: an introduction to fractional derivatives, fractional differential equations, to methods of their solution and some of their applications. 1998 (198): Academic press.

44. Honig G, Hirdes U. A method for the numerical inversion of Laplace transforms. Journal of Computational and Applied Mathematics. 1984 (10): 113–132. doi: 10.1016/0377-0427(84)90075-X

45. Vieira Neto J, Martins A,Ataíde C, Barrozo M. The effect of the inner cylinder rotation on the fluid dynamics of non-Newtonian fluids in concentric and eccentric annuli. Brazilian Journal of Chemical Engineering. 2014 (31): 829–838. doi: 10.1590/0104-6632.20140314s00002871

46. Orczykowska M, Dziubinski M. The fractional derivative rheological model and the linear viscoelastic behavior of hydrocolloids. Chemical and Process Engineering. 2012 (33): 141–151. doi: 10.2478/v10176-012-0013-2

47. Navarrete R, Himes R, Seheult J. Applications of xanthan gum in fluid-loss control and related formation damage. SPE Permian Basin Oil and Gas Recovery Conference, Society of Petroleum Engineers. 2000.

48. Sherief HH, Elmisiery A, Elhagary M. Generalized thermoelastic problem for an infinitely long hollow cylinder for short times. Journal of Thermal Stresses. 2004 (27): 885–902. doi: 10.1080/01495730490498331